Available online at
www.ijacskros.com

Indian
Journal of Advances in
Chemical Science

Indian **J**ournal of **A**dvances in **C**hemical **S**cience **1** (2012) 1-9

Groundwater Geochemistry Study of Estuarine Aquifer, Western India: Mumbai using Chemometric and Conventional Techniques

Sabyasachi Rout*, **Ajay Kumar, P.K. Sarkar, Manish K. Mishra, P.M. Ravi**

Health Physics Division, Bhabha Atomic Research Centre, Mumbai, India-400085

Received 25 October 2012; Accepted 5 November 2012; Available on line December 2012.

ABSTRACT

A hydrogeochemical study of an estuarine aquifer system was carried out to find significant processes controlling groundwater geochemistry. The data interpretation was carried out using both conventional as well as chemometric techniques. Piper's Trilinear diagram identified (Na+K)–(SO_4+Cl), (Ca+Mg)–(SO_4+Cl) and (Ca+Mg)–HCO_3 as predominating hydrochemical facies of the area. Both Gibbs classical diagrams and stability diagrams revealed that rock weathering as the important geochemical process controlling the groundwater chemistry rather than atmospheric precipitation although the study site is under high rainfall. Stability diagram and hydrochemical indices study ruled out the seawater intrusion to the aquifer. Kaolinite was found to be predominating clay mineral of the site. Chemometric analysis like Factor analysis of hydrochemical data, extracts three hydro-chemically meaningful factors which includes both natural and anthropogenic origin.

Key words: *Ulhas Estuary, Saline intrusion, Kaolinite, Hydrogeochemistry, Factor Analysis, Piper Trilinear Plot, Stability Diagram.*

1. INTRODUCTION

Estuaries occupy the boundaries between terrestrial and marine systems. Chemical characterization of groundwater of estuarine aquifer is very complex as it is influenced by two environments such as river and sea. At present there is a great threat of seawater intrusion to the coastal as well as estuarine aquifers which will become more problematic in future due to over exploitation of groundwater coupled with rise in mean sea level. In recognition of their importance to the health of coastal habitats, it is important to monitor the water quality and study its hydrogeochemistry. The natural composition of the groundwater is determined by chemical analysis; the data from which may be grouped or statistically evaluated. Several hydrochemical code (PHREEQC, WATCLAST, etc.) and graphical methods like Piper Trilinear diagram, Durov diagram etc. are used for visualization and classification of hydrochemical data but they are limited to major constituent ions and ignore many parameters which are otherwise important for studies. Hence, with increase in complexity of chemical and physical evolution of groundwater and number of data/or parameters these models are unable to draw a clear picture of hydrochemical process underlying in the system under study [1]. Multivariate data exists in multidimensional space which is clearly impossible to visualize above 3D. In order to handle large set of data or parameters simultaneously and to get reliable interpretation, multivariate statistical techniques such as factor analysis (FA) and cluster analysis (CA) have been used successfully in environmental studies. These statistical techniques can provide a powerful tool for analyzing the multivariate geochemical data of groundwater. The factor analysis is used to simplify the complex and diverse relationships which exist among a set of observed variables by interrelating common and unobservable factors. It also explains the correlations between the variables in terms of the underlying factors, which are not apparent. Usually, in environmental studies FA is used to identify the sources of pollutants and their contribution [2].

This work was a joint approach of conventional and advanced chemometric techniques to study groundwater geochemistry of estuarine aquifer system. Hydro-geochemical model like PRHEEQC and graphs like Piper's Trilinear diagram, Gibbs Boomerang diagram and thermodynamic stability diagrams were used to assess the geochemical processes. FA was carried out to establish the relations, associations (geological origin) between the parameters, and to find out the link between different locations of observation area based upon similarity in geochemical evolution. In addition to this it also identified external factors (anthropogenic) influencing the system. In this study, STATISTICA software package (Stat soft India, ver. 7) was used for the basic statistical analyses, correlation matrix and factor analysis.

2. MATERIALS AND METHOD

2.1 Study area

The study area is located in the northern part of Mumbai between latitude $19^0\ 16^{'}75^{''}$ N- $19^0 23^{'}14^{''}$ N and longitude 72^0 44'98$^{''}$E-72^0 56'56$^{''}$E is an

---

*Corresponding Author:
Email: srout.barc@gmail.com
Phone: +91-022-25592653;
Fax No: 022-25505151

estuarine area. The estuary is formed by the Ulhas River which originates from Western Ghats and meets the Arabian Sea forming an estuary about 3 km wide at Vasai. The physiographic feature of the study area is broad and flat terrain (7-20.7 m above msl) flanked by north–south trending hill ranges (100-625 m above msl). The average temperature remains about 25 ^{0}C. The average annual rainfall in this region is 2170 mm. The study site has a highly humid climate with an annual average relative humidity of more than 60%. As per the Central Ground Water Board, India the study area is underlain by basaltic lava flows of upper Cretaceous to lower Eocene age. The shallow alluvium formation of recent age also occurs, as a narrow stretch, along the river flowing in the area. From mineralogical point of view the study area is fine grained, dark greyish to greenish in colour and consists of predominately augite and calcic plagioclase with minor olivine. The site is dominated with clay minerals like montmorillonite, kaolinite and illite [3].

2.2 Sampling

A grid sampling scheme was prepared with the help of topocity map for a total area of about 200 km^2 on both sides of the creek (Figure. 1) with sub grid dimension of 4 km × 2 km. The study site was classified into 25 sub locations. Sampling was carried out in the summer season in the month of March to April. Two aliquots of groundwater samples from each hand dug wells were collected and filtered through 0.45 micron cellulose acetate membrane (Millipore Corporation) and stored in, acid washed, 200 ml capacity polypropylene bottles. One of the aliquot was acidified with 0.01M of nitric acid (AR Grade, Merck, India) and samples were kept in refrigerator at a temperature of 4^{0}C till analysis.

2.3 Analysis Techniques

Field measurements consisted of unstable parameters like temperature, electrical conductivity (EC) and pH were measured using *AQUA Read meter* (UK) with AP-1000 prob. Major ions like Na^+, K^+, Mg^{2+}, Ca^{2+}, F^-, Cl^- and SO_4^{2-} in groundwater samples were estimated by conductivity suppressed *Ion-Chromatography* System (DIONEX600, USA). Bicarbonate (HCO_3^-) was estimated titrimetrically using autotitrator (Metrohm-798 MPT Titrino, Switzerland). Silica (Si) in groundwater was determined by Atomic Absorption Spectrophotometer (GBC Avanta, Australia). The quality assurance was made by spike recovery, replicate analysis and cross method checking. Measurement of Cu, Fe, Mn and Pb in water samples was carried out using mixed bed ion-exchange column (CS5A, Dionex, USA) using oxalic acid and pyridine-2,6-dicarboxilic acid (PDCA) as eluent as per standard method [4]. The detection has been accomplished using 4-(2-pyridylazo)-resorcinol (PAR) as post-column reaction agent and absorbance monitoring at 530 nm.

All measurements were performed in duplicate, with relative errors between 2- 5%. Total dissolved solids were calculated using the ionic concentrations of different ions.

3. RESULTS AND DISCUSSION

3.1 Hydrogeochemistry of groundwater

The summary of the analytical results of ground water in the study area and their descriptive statistics is presented in Table 1. Standard deviation (SD) and percentage of coefficient of variance (%CV) represents the dispersion of the data. The %CV for all parameters, except pH, showed very wide variation (43 to 235.0%) indicating that there was non-homogeneity in the distribution of ionic contents throughout the study area. This wide spread of data may be accounted to weathering processes, and anthropogenic input etc. The pH of groundwater samples ranged from 6.25 to 8.1 with an average of 7.36 (slightly alkaline). Higher pH values of groundwater at few locations may be due to weathering of plagioclase feldspar by dissolved atmospheric carbon dioxide that releases Na^+, Ca^{2+} and HCO_3^- which progressively increases the pH of water [5]. A high mean ratio (> 2) of Ca to Mg was observed in groundwater indicating that incongruent dissolution of calcium bearing silicate minerals like Ca- plagioclase might have taken place.

The ratio of HCO_3^- to dissolved silica in groundwater was found to be high (>10), and this supports that plagioclase weathering was the major water–rock interaction of the site. Some samples of groundwater showed a high mean ratio (>1) of Na to Cl indicative of Na released as a result of incongruent dissolution of sodium bearing silicate minerals like sodium plagioclase or may be due to cation exchange with sodium clay from basalt alternation [5].The mean value of EC and TDS of groundwater samples were 1257.39 µS/cm and 745.3 mg/L respectively. Higher values of electrical conductivities recorded in groundwater at few locations may be due to seawater influence as the area is nearby Arabian Sea. This can be verified from the ionic relations and other hydrochemical studies (thermodynamic stability diagram). The following ionic relationships were contemplated to check the salinity and origin of the groundwater in

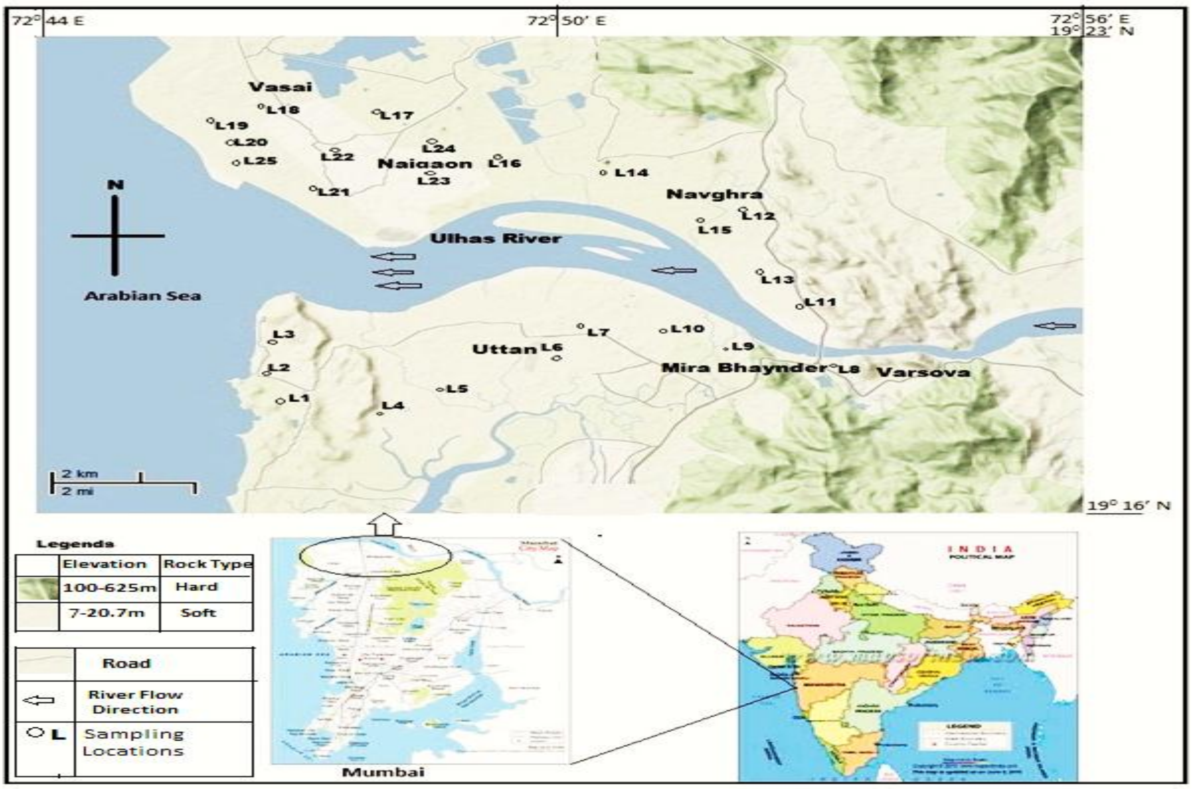

Figure. 1: Map of the groundwater sampling locations in the estuarine region of Mumbai

the study area. These includes: Mg/Ca, Cl/HCO_3, and the Cationic Exchange Value (CEV = [Cl^- (Na + K)]/Cl). Mg/Ca values were all less than 2.0 (Table 2) i.e. ranging 0.15 - 1.66. As inferred from this index, the groundwater in the area appears to be inland in origin, because waters under the influence of sea would have values of about 5 except where other processes such as cationic exchanges intervene; the values could be 4 or less [6, 7]. In general, the CEV for seawater ranges from +1.2 to +1.3 [8]. The CEV values for groundwater of study site were below 1.0 (Table 2) ranging from -2.41 to 0.92, indicating that the groundwater was inland in origin.

The Cl/HCO_3 values range from 0.14 - 13.21 (See table 2) with 22 locations having values <5 and remaining three locations between 5 -20 (figure 2). The values of hydro geochemical index given for fresh waters are between 0.1 and 5 and for seawater between 20 and 50 [9]. Considering above ionic relations it may be assumed that saline intrusion is not the reason for high EC and TDS of few locations. Other mineralogical evidences for ruling out the saline intrusion are discussed in coming sections.

3.2 Piper's groundwater's classification

Figure 3 is the Trilinear Piper's plot for groundwater classification of the study site. The geochemical evolution of groundwater can be interpreted by plotting the concentrations of major cations and anions in the Piper Trilinear diagram. In this diagram, cations and anions were normalized to 100% and plotted in their appropriate triangle. The main function of the Piper diagram is to identify the hydro-facies, nevertheless, it also help us to understand the several geochemical processes along the flow path of the groundwater. The plot showed that, groundwater of 7 locations were strongly alkali type (Na^++ K^+ > 50 % of total cationic composition), 18 locations were of Ca^{2+} type (Ca^{2+}+Mg^{2+}> 50 % of total cationic composition). Similarly for anions, groundwater of 9 locations were of bicarbonate type (HCO_3> 50 % total anionic composition), 16 were of $Cl-SO_4$ type. On this basis, groundwater was also classified into three dominant chemical facies of (Na+K)–(SO_4+Cl) type, (Ca+Mg)–(SO_4+Cl) type and (Ca+Mg)–(HCO_3) type. Hence, for Ca^{2+} - Mg^{2+} type water there are 18 locations (1, 4, 5, 8, 9, 10, 12, 13, 14, 15, 16, 17, 19, 20, 21, 22, 23 and 24) which can be divided as follows:

18= 10 (With anions SO_4^{2-} and Cl^-) + 8 (With anion type CO_3^{2-} and HCO_3^-)

And rest seven locations (2, 3, 6, 7, 11, 18, and 25) belong to Na^+ -K^+ water type with anions as follows:

7= 6 (With anions SO_4^{2-} and $Cl^{-)}$ +1 (With anion type CO_3^{2-} and HCO_3^-)

Table 1. Summary statistics data of groundwater of Ulhas estuarine aquifer of analytical.

Geochemical Parameters	Mean	Median	Minimum	Maximum	IQR	SD	% CV
Cl (mg/L)	260.85	84.36	12.36	1960.88	161.81	486.78	186.61
SO_4^{2-}	64.580	34.48	2.52	543.59	27.67	117.01	181.18
Na	136.29	31.64	9.07	1493.84	96.79	299.76	219.94
K	6.436	3.16	0.59	21.27	7.74	6.48	100.68
Mg	16.258	10.31	3.98	76.01	11.14	17.98	110.59
Ca	59.51	64.77	13.78	138.47	44.48	32.42	54.48
pH	7.36	7.39	6.25	8.10	0.535	0.464	6.30
HCO3	142.89	133.66	40.23	323.4	73.23	61.97	43.36
Si	4.115	3.73	1.17	10.17	1.69	2.13	51.76
TDS	745.30	484.07	116.12	3767.9	466.19	841.53	112.91
EC (µS/cm)	1257.39	810.0	181	5890	962.00	1314.65	104.55
Cu(µg/L)	4.682	2.0	1.0	24	3.20	6.00	128.15
Fe	40.66	46.5	1.2	116	42.30	26.18	64.38
Mn	58.48	17.3	2.0	557.1	11.05	137.44	235.02
Pb	33.520	1.2	0.46	101.0	100.00	47.31	141.13

Table 2. Ionic Relation of Ground Water

Location	**Cl/HCO3**	**CEV**	**Mg/ Ca**
L1	2.8	-0.34	1.66
L2	2.4	-1.38	0.27
L3	12.7	0.80	0.24
L4	0.15	-2.14	0.15
L5	0.76	-1.16	0.35
L6	2.1	-0.66	0.76
L7	13.4	-0.36	0.91
L8	2.7	0.87	0.35
L9	0.23	-1.37	0.19
L10	2.1	0.56	0.35
L11	4.3	0.24	0.64
L12	0.39	0.21	0.35
L13	1.12	0.48	0.41
L14	0.65	-0.23	0.35
L15	0.14	-0.15	0.49
L16	0.46	-0.43	0.30
L17	1.15	0.50	0.22
L18	0.97	-1.21	0.48
L19	1.65	0.34	0.29
L20	0.56	0.27	0.39
L21	0.84	0.16	0.34
L22	1.05	0.46	0.43
L23	0.57	-0.68	0.19
L24	5.98	0.92	0.25
L25	3.01	0.19	0.51

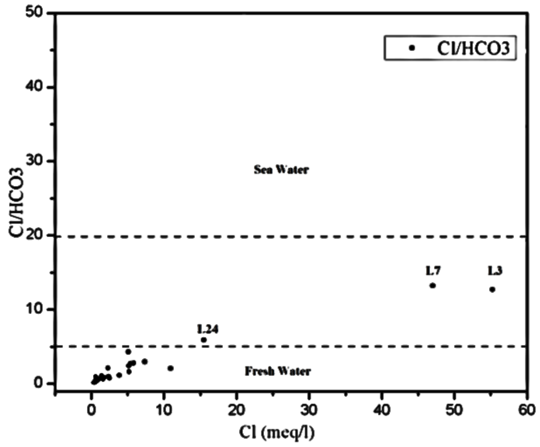

Figure 2. Ionic ratio of Cl/HCO3 versus Cl concentration (meq/l).

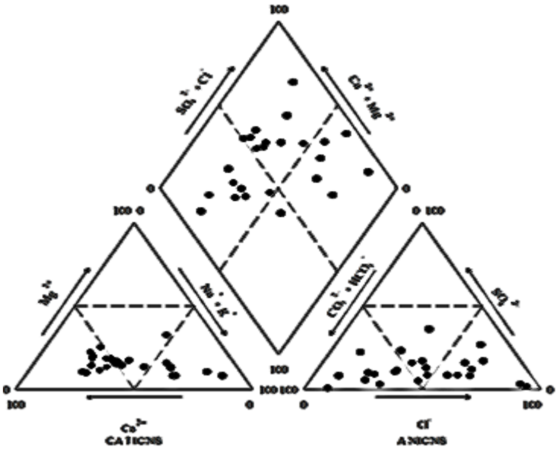

Figure 3. Trilinear Piper's plot for groundwater classification of sampling site

3.3 Gibbs boomerang diagram

Gibbs boomerang diagram is one of the important tools to investigate geochemical processes. Gibbs identified three natural mechanisms control the waters chemistry: atmospheric precipitation, rock weathering, and evaporation-crystallization process. Gibbs' diagram, a boomerang-shaped envelope, is obtained when the weight ratio Na/ (Na+Ca) on the X axis is plotted against TDS values on the Y axis and the same goes for anions Cl/ (Cl+HCO_3) vs TDS (see figure 4(a) and 4(b)).When the dominant process is rock weathering, waters produce Ca^{2+} and HCO_3^- as predominant ions, TDS values are moderate and sample data plot lies in the middle region of the Gibb's boomerang. Low salinity waters of sodium chloride type are due to the atmospheric precipitation processes and sample data plot lies in the lower right corner of the boomerang. The third mechanism that controls the water chemistry is the evaporation–crystallization process which is important in arid regions, where evaporation is higher than precipitation. When the weight relation Na/(Na+Ca) was plotted against TDS values for the estuarine system waters under study, it was ascertained that ground water of the 4 locations lies outside the boomerang. Where Na/(Na+Ca) values lay between 0.6 and 1.0 and TDS values between 6.0-50.0 g L^{-1} (figure 4(a)). This indicates that, rock weathering and evaporation-crystallization processes alone are unable to explain the chemical characteristics of ground water of these 4 locations. On the other hand, the plot of Cl/ (Cl+HCO_3) vs TDS (Y axis) values (figure4b) exhibits similar distribution pattern like cationic diagram i.e., four locations are out of the boomerang envelop and remaining locations were under rock weathering dominance region.

As per Drago and Quiros [10] deviation from Gibb's general pattern arises due excess dissolution of salt (halite) and/or ion exchange reactions (i.e., sodium clay interacts with a solution rich in calcium, each couple of adsorbed sodium replaced by a solubilised calcium, which enriches groundwater in sodium, thus changing it from calcium bicarbonate to sodium bicarbonate type). In order to explain the origin of the excess of Na, a plot of (Ca+Mg)-(SO_4+HCO_3+CO_3) against (Na–Cl) in meq/l was performed (See figure 5). Results indicated a weak negative correlation (R^2= -0.02) and a slope (0.033) which is far from the theoretical value of -1 for ion exchange reaction [11]. This is against the assumption of ion exchange causing the deviation. The above result led us to assume that rock weathering is the important process controlling the chemistry of the water with few locations affected halite dissolutions as same numbers of locations were exhibiting deviation in both the cation and anion diagram of Gibbs-boomerang.

3.4 Stability diagrams of clay minerals in groundwater system

Stability diagrams are graphical representations of equilibrium between minerals and aqueous solutions. Such diagrams are very useful in deducing what will happen when waters of various compositions interact with solid phases. The stability diagrams for the groundwater of different locations are presented in the figure 6 (a-d) for K, Na, Ca, Mg-systems respectively. The phases of interest in aqueous system were Gibbsite, Kaolinite, Na-montmorillonite and Feldspar. All the stability diagrams showed that kaolinite was thermodynamically more stable in the groundwater environment of the site although gibbsite is expected in such type of equilibrium as end product. This indicates low infiltration of rain water into groundwater, hence low flushing rate. $[M^+]/[H^+]$ ratio (where, M^+ can be K^+, Na^+, Ca^{2+}, Mg^{2+}) and H_4SiO_4 concentration relates to flushing rate. Increase in flushing with rain water due to good infiltration causes decrease in the $[M^+]/[H^+]$ ratio and concentration of silicic acid. The dominancy of kaolinite indicates low flushing at region otherwise gibbsite found to be predominate at the site.

In K-System, (figure 6 (a)) the conversion of K-feldspar to kaolinite involves consumption of H^+ and release of K^+ and H_4SiO_4. K^+ can also be incorporated into the formation of more K-feldspar, illitic mica, or the mixed-layer clay illite or smectite [12]. Akin to K-system in other systems like: Na- system (Na-Montmorillonite to Kaolinite Figure 6 (b)); Ca-System (Ca-Montmorillonite to Kaolinite, figure 6 (c)), and Mg- System (Chlorite to Kaolinite; figure 6 (d)) all the systems involve consumption of H^+ and release of Ca^{2+}, Na^+ and Mg^{2+} ions followed by silicic acid. Gibbsite which was formed by decomposition of kaolinite is highly unstable and readily converted to Kaolinite as soon as gibbsite to kaolinite boundary is encountered. The plausible weathering reactions are presented as follows.

Weathering Reactions:

a) *K- feldspar to Kaolinite*

$$2KAlSi_3O_8 + H^+ + 9H_2O \leftrightarrow A1_2\,Si_2O_5\,(OH)_4 + 2H_4SiO_4 + 2K^+$$

b) *Na- Montmorillonite to Kaolinite*

$$Na_2Al_{14}Si_{22}O_{60}\,(OH)_{12}\ \textit{(Na- Montmorillonite)} + 2H^+ + 23H_2O \leftrightarrow 7Al_2Si_2O_5\,(OH)_4 \textit{(Kaolinite)} + 8H_4SiO_4 + 2Na^+$$

c) *Ca-Montmorillonite to Kaolinite*

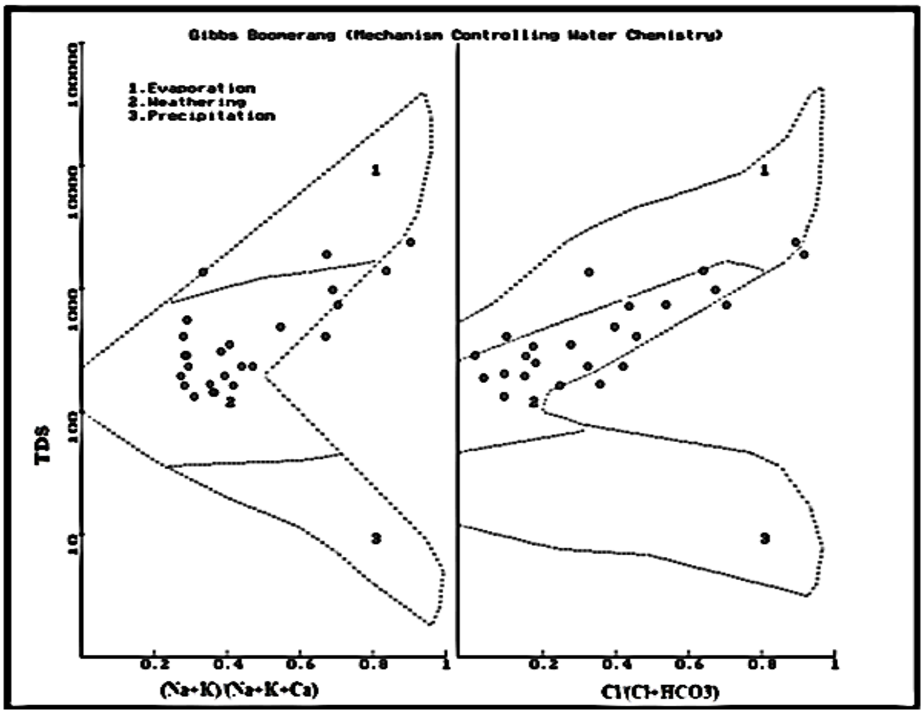

Figure 4: Gibbs Boomerang diagram of groundwater (a) Gibbs cationic diagram (b) Gibbs-anionic diagram

$CaAl_{14}Si_{22}O_{60}(OH)_{12}$ (Ca-Montmorillonite) + $2H^+$ + $23H_20 \leftrightarrow 7Al_2Si_2O_5(OH)_4$, (Kaolinite) + $8H_4SiO_4 + Ca^{2+}$

d) Chlorite to Kaolinite

$(Mg_5Al)(AlSi_3)O_{10}(OH)_8$ (Chlorite) + $10H^+ \leftrightarrow$ $Al_2Si_2O_5(OH)_4$(Kaolinite) + $8H_4SiO_4 + 5Mg^{2+}$

e) *Kaolinite- Gibbsite reversible reaction.*

$A1_2Si_2O_5(OH)_4$ (Kaolinite) $+5H_20 \leftrightarrow A1_2(OH)_6$ (Gibbsite) + $2H_4SiO_4$

The climatic condition of Mumbai, which is tropical wet/humid, also favours the dominance of the kaolinite, as under humid climates kaolinite is considered to be stable clay mineral [13]. Absence of muscovite at sampling site indicates that there was no interaction between groundwater of the aquifer and sea water. As Clay minerals (e.g. kaolinite) in contact to sea water tend to take up K^+ from sea water and are converted to muscovite. Study of stability diagram also confirms the assumption made on the basis of Gibbs diagram, i.e., weathering is predominate process controlling hydrogeochemistry rather than atmospheric precipitation.

3.5 Multivariate Statistical Analysis of water

3.5.1 Factor analysis

In order to find most significant processes controlling chemistry of the groundwater considering all the major and minor parameter simultaneously, factor analysis was carried out. Factors were extracted using principal components extraction method and subjected to varimax normalization rotation for better interpretation. Factor analysis extracts four factors (Factor having Eigen value >1 and loading >0.6) which is accounted for 80.61% variance of the total variance (see table 3). Therefore, these four factors were assumed to represent adequately the overall variance of data set. Table 4 presents the factor loading matrix. Table 3 and 4 showed that 3 factors out of four were hydrochemically meaningful, which seemed to describe the existing conditions of groundwater chemistry.

The first factor (F1) with 34.68% of variance comprises Cl, Na, Mg, and Ca with high loadings this associations strongly suggests that these variables have similar source. The source could be either lithogenic in origin (weathering of soil minerals) or seawater intrusion. But seawater intrusion can be rejected because locations from 1 to 5 were moderately affected by F1 and locations 20 to 25 least affected, although these locations are neared by sea. On the other hand location 7 is highly affected by F1 (Factor score-4.15, figure 7 (a)) situated far away from seawater line. Hence considering above fact and looking at topographic condition of the study site discussed earlier in section 2.1, stability diagrams and hydrogeology of the area i.e., alluvium aquifer along the river and costal area of the study site have high fresh water potential, F1 was assumed to be of purely lithogenic origin.

The second factor 2 (F2), contributes Cu, Mn and Pb at 20.44% variance. A good degree of correlation between Cu, Mn and Pb revealed that

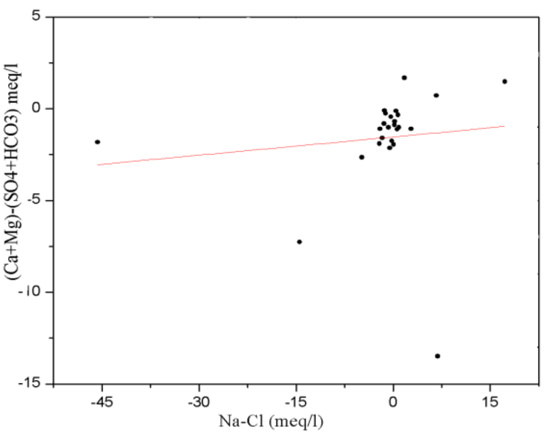

Figure 5. Ionic Relation Plot for groundwater of study site.

these species have common source of origin and arisen from anthropogenic activities. The factor (F2) score plot (See figure 7 (b)) indicates that, almost all the locations were unaffected by this factor except location numbers 1, 6, 8 and 16, where these sites were situated nearby highway. This strongly supports that F2 attributed due to vehicular activities. Factor 3 (F3) accounted for the 14.03% of total variance and loaded positively with K^+ and negatively with Si and Fe. Negative loadings of Fe and Si signify that there occurs incongruent weathering of jarosite-K. This is the weathered product of basalt due to water rock interaction. Jarosite-K is very unstable in humid condition which rapidly decomposes to produce ferric oxihydroxide i.e., goethite [14].

Facts in support of Jorasite-K decomposition were: a) PHREEQC simulation study revealed that, all the locations were over saturated w.r.t goethite ($SI_{Goethite}$ is ≥ 4.27) and under saturated w.r.t Jorasite-K ($SI_{Jorasite-K}$ is ≤ -5.68) b) predominance of kaolinite (figure 6), as under most conditions jarosite is accompanied by kaolinite and gypsum [14] and c) hydrological study revealed that, groundwater of study area exists in fractures, joints, vesicles and in weathered zone of Basalt.

Hence, F3 could be considered as decomposition of Jorasite-K and locations significantly affected by F3 were 1 to 6, 12, 17, 19 and 20 (See figure 7(c)). Factor 4 (F4) alone explains 15.13% of the variance of our result this factor can be pooled variable. It is more difficult to ascertain the physicochemical meaning of this pooled variable. Locations affected by factor four were 6, 8 and 24 (figure 7(d)).

4. CONCLUSION

The principal geochemical processes determining the chemical composition of estuarine aquifer were studied using both conventional as well as chemometric techniques. Interpretation of hydrochemical data using Piper diagram identified three dominant hydrochemical facies of (Na+K)–(SO_4+Cl), (Ca + Mg) – (SO_4+Cl) and (Ca+Mg)–HCO_3 types. When geochemical processes were analyzed through Gibb's boomerang diagram and stability diagrams, weathering came out as an important geochemical process which determines the chemistry of the groundwater of the site rather than atmospheric precipitation though the study area is under heavy rainfall. Kaolinite was found to be the predominating clay mineral of the site.

Chemometric study of parameters provides a compressive idea about the hydrochemical processes and groundwater evolution of study site which were previously interpreted individually by different models and diagrams. It allows geochemical zonation of aquifer systems which takes into account effects of lithology, anthropogenic and hydrogeology context when dealing with aquifer systems. Factor analysis extracted three meaningful factors controlling the hydrogeochemistry of groundwater of the study area. They were, weathering process (lithogenic), anthropogenic inputs of heavy metals and weathering of Jarosite-K.

The ionic relation and hydrogeochemical model studies indicate that there is no threat of saline intrusion to the estuarine aquifer. The results are important not only in local aspects as they allow a quick response to finding solutions but also in broader sense to provide an idea about the estuarine aquifer under the influence of two types of water bodies i.e. sea and river.

Table 3. Eigen value for factor analysis of ground water.

Fac tors	**Eigen value**	**% Total variance**	**Cumulative Eigen value**	**Cumu lative %**
1	4.16	34.68	4.16	34.68
2	2.64	22.0	6.80	56.69
3	1.82	15.13	8.62	71.83
4	1.05	8.78	9.67	80.61

Acknowledgements

The authors sincerely acknowledge the guidance and help provided by Dr. A.G. Hegde and Dr. Usha Narayanan, ESS, Health Physics Division, Bhabha Atomic Research Centre, Mumbai.

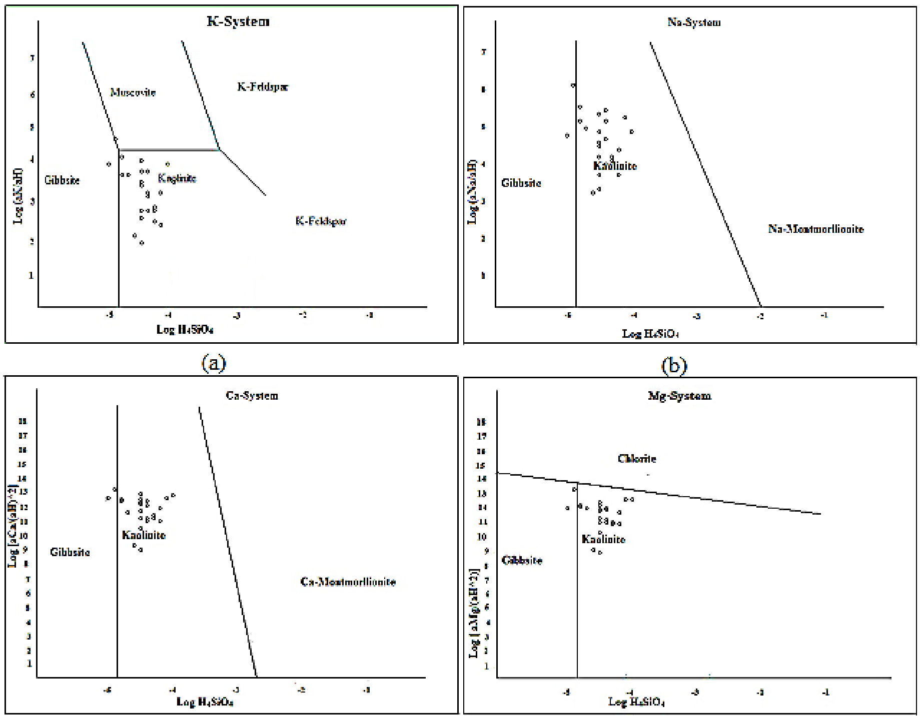

(a) (b)

(c) (d)

Figure 6. Thermodynamic stability diagram of a) K-System, b) Na-System, c) Ca- System and d) Mg-System

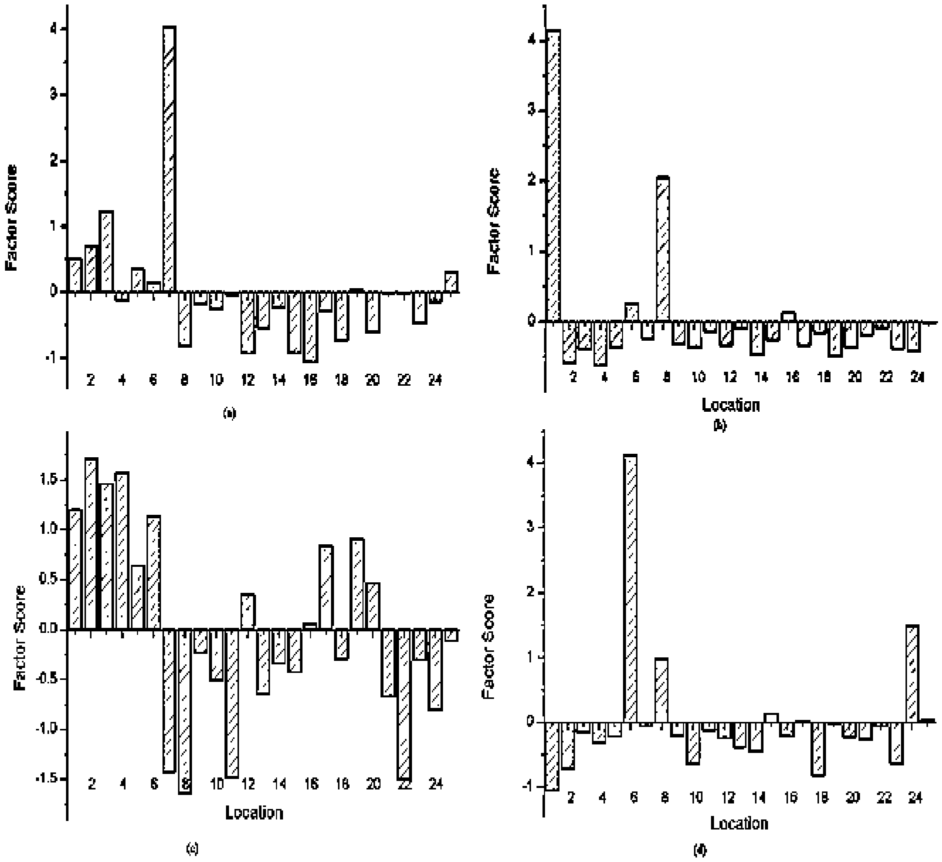

Figure 7. Factor score plot of, a) Factor-1, b) Factor-2, c) Factor-3 and d) Factor-4

Table 4. Factor loading matrix of groundwater

Variables	Factor 1	Factor 2	Factor 3	Factor 4
Cl^-	0.779	-0.040	0.048	0.141
SO_4^{2-}	0.112	0.040	0.061	0.927
Na^+	0.918	0.008	-0.096	0.153
K^+	0.576	0.085	0.643	0.258
Mg^{2+}	0.810	0.482	0.044	0.060
Ca^{2+}	0.838	-0.131	0.338	0.046
HCO^-_3	0.391	-0.069	0.423	0.656
Si	-0.108	-0.010	-0.774	-0.031
Cu	-0.063	0.817	0.013	0.415
Fe	0.499	-0.210	-0.629	-0.219
Mn	-0.063	0.956	-0.033	-0.043
Pb	0.142	0.873	0.168	-0.187

5. REFERENCES

[1]. K. R. Karanth., (1987) Assessment development and management of groundwater; Tata McGraw Hill: New Delhi.

[2]. S. A. Mahamoud, A.S. Abdullah, (2009) Determination of dominant chemical processes in an alluvial aquifer system of Wadi Ghiran using Multivariate statistical Analysis, ***Earth Scence.,*** **20,** 1-10.

[3]. D. S. Rath, S. K. Sahu, (1993) Source And Distribution of metals in Urbann soil of Bombay, India, using multivariate statistical techniques, ***Environmental Geology,*** **22,** 276-285.

[4]. M. M. Sandro, R. Selvaggi, A. Poletti, (2011) Determination of trace transition metals in environmental matrices by chelation chromatography, ***Environmental Monitering and Assessesment,*** **174,** 313-326.

[5]. G. N. Eby., (2004) Principles of Environmental Geochemistry; Thomson learning academic center:USA.

[6]. V.V.J. Sarma, N. Krishnaiah, (1976) Quality of groundwater in coastal aquifernear Visakhapatnam, India, ***Groundwater,*** **14**, 290-295.

[7]. P. Pulido-Leboeuf, A. Pulido-Bosch, M. L. Calvache, A. Vallejos., J. M. Andreu, (2003) Strontium, SO4$^{2-/}$Cl^{-} and Mg^{2+}/Ca^{2+} ratios as tracers for the evolution of seawater into coastal aquifers: the example of Castell de Ferro aquifer (SE Spain). C. R, ***Geoscience,*** **335,** 1039-1048.

[8]. E. Custodio, M.R Llymas., (1983) Hydrologia Subterranean; Omega: Barcelona.

[9]. E. Custodio, (1987) Groundwater problems in coastal areas, In; Studies and Reports in Hydrology: UNESCO.

[10]. E. Drago, OS. R. Quir, (1996) The hydrochemistry of the inland waters of Argentina: a review, ***International Journal of Salt Lake Research,*** **4,** 315-325.

[11]. S. Fisher, W. Mullican, (1997) Hydrochemical evolution of sodium sulfateand sodium- chloride groundwater beneath the Northern Chihuahuan desert, Trans-pecos, TX, USA, ***Hydrogeology Journal 5,*** 4-15.

[12]. P.W. Birkeland., (1999) Soils and geomorphology; Oxford University Press: New York.

[13]. G.D. Price, A. H. Ruffell, C. E. Jones, R. M. Kalin, J. Mutterlose, (2000) Isotopic evidence for temperature variation during the early Cretaceous (late Ryazanian-mid-Hauterivian), ***Journal of the Geological Society, London,*** **157**, 335-343.

[14]. D. Langmuir., (1999) Aqueous Environmental Geochemistry; Prentice Hall: New Jersey.

****Biographical Sketch***

***Sabyasachi Rout** did his Bsc and MSc. in Chemistry from Utkal University, Odisha, India. Then he has joined Bhabha Atomic Research Centre as Scientific Officer in the year 2009 after successful completion of the one year Orientation courses in Nuclear Science and Engineering from Training School BARC Mumbai. He did his M. Tech. in Radiological Safety Engg. with specialization in Nuclear Engineering from Homi Bhabha National Institute Mumbai. As a major part of his research work, he is actively involved in the Environmental speciation modeling of heavy metals, Chemometric study for source apportion or receptor modeling. He is also actively involved in the radiological dose apportion due to normal operation of Nuclear Power Plants, and development of analytical methods for trace level estimations of heavy metals in different environmental matrices using Voltammetry and Ion-Chromatographic techniques.*